SUPPLEMENTARY MATERIALS AND METHODS

Fluorescence correlation spectroscopy (FCS)

The FCS signal originates from the transits of fluorescently tagged molecules through a confocal detection volume at low concentration, which create fluctuations in the detected fluorescence intensity in a manner dependent on the underlying molecular kinetics (1). The fluorescence intensity fluctuations $\delta I(t)$, resulting from the fluorescent molecules transiting through the confocal volume, when correlated with fluorescence intensity fluctuations detected after time $(t + \tau)$ yield the normalized intensity autocorrelation function $G(\tau)$:

$$G(\tau) = 1 + \frac{< \delta I(t)\delta I(t+\tau) >}{< I >^2} \quad (1)$$

where the angled brackets describe the time-average and $<I>$ the mean fluorescence intensity (2,3). For the cell measurements performed in this work a standard two-component diffusion autocorrelation function in a 3-D Gaussian focal volume was used (4):

$$G(\tau) = \frac{1}{N}\left[\frac{F_1}{\left(1+\frac{\tau}{\tau_{D_1}}\right)\left(1+\frac{\tau}{s^2\tau_{D_1}}\right)^{1/2}} + \frac{F_2}{\left(1+\frac{\tau}{\tau_{D_2}}\right)\left(1+\frac{\tau}{s^2\tau_{D_2}}\right)^{1/2}}\right] \quad (2)$$

S is the structure parameter, $S = \omega_z / \omega_0$, where ω_0 denotes the $1/e^2$ radius of the 3D Gaussian confocal volume, ω_z is axial radius of confocal volume. The two components F_1 and F_2 represented a fast, freely-diffusing, fraction and a slower-moving fraction, respectively, which is thought to interact with nuclear structures and is more vulnerable to photobleaching. The mean molecular transit time through the confocal observation volume for each of these diffusing components is given as (5,6):

$$\tau_{D_i} = \omega_0^2 / (4D_i) \quad (3)$$

τ_{Di} being the diffusion time and D the diffusion coefficient for $i=1,2$ the fast and slow components, respectively. The average number of molecules, N, in the confocal volume is given by (4):

$$N = CV_{eff} \tag{4}$$

where C is the concentration and the effective confocal volume, $V_{eff} = \pi^{3/2} S\omega_0^3$.

FCS measurements were performed using the ConfoCor3 attachment of a LSM 510 META confocal microscope, (Version 4.2, Carl Zeiss MicroImaging GmbH, Jena, Germany) with a 40x water immersion C-Apochormat objective lens with a N.A. of 1.2. Calibration of the confocal volume size for the green channel was performed using 4 nM of Rhodamine 6 Green placed inside eight-well Lab-Tek chambered borosilicate coverglass chambers (Nalge Nunc International, Rochester, NY). Using the known diffusion coefficient of 2.8 x 10^{-10} m^2/s for this fluorophore and fitting to a one-component diffusion model (7) resulted in a confocal volume 0.34 fl. Specifically, the radial axis dimension, ω, was 0.23 μm and the axial dimension z was 1.15 μm, making S equal to 5. For Xrs6 cells expressing GFP-Ku80, measurements were obtained using the 488 nm argon laser line with ~4 μW at the focal spot. A dichroic mirror (HFT 488/543) was used for separating the laser excitation beam from the collected fluorescence emission, and an excitation cut-off filter (NFT 500) was used before signals were directed to an avalanche photodiode (APD) detector. For V3 cells expressing YFP-DNA-PKcs, measurements were obtained with the 514 nm argon laser with ~3 μW at the focal spot. In this case, a different dichroic mirror (HFT 458/514) was used to separate laser excitation from fluorescence emission, and a band pass filter (BP 530-610 IR) was used to shield the APD from any excitation light leakage.

SUPPLEMENTARY RESULTS

Figure S1: Single point FCS measurements induce photobleaching when performed repeatedly at different time points post-irradiation. (**A-E)** Confocal images of an Xrs6 cell expressing GFP-Ku80 when consecutive point FCS measurements are performed and **(F-J)** when consecutive RICS experiments are performed. Application of N&B analysis also showed very little bleaching after repeat measurements (not shown).

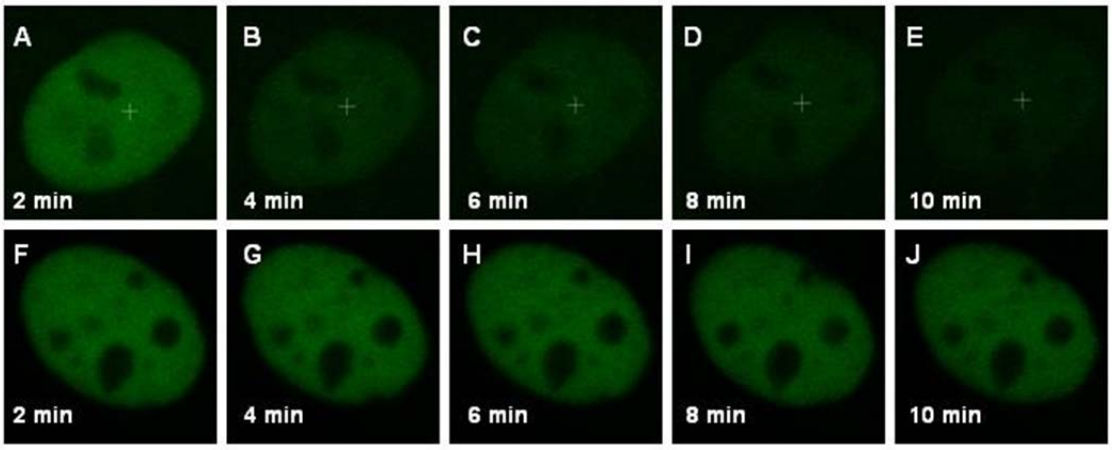

Figure S2: Molecular brightness values as a function of time post-irradiation were constant for both GFP-Ku80 (**A**) and YFP-DNA-PKcs (**B**), independent of γ-irradiation dose. Each data point shows the mean and standard deviation of brightness measurements from 10 cell nuclei.

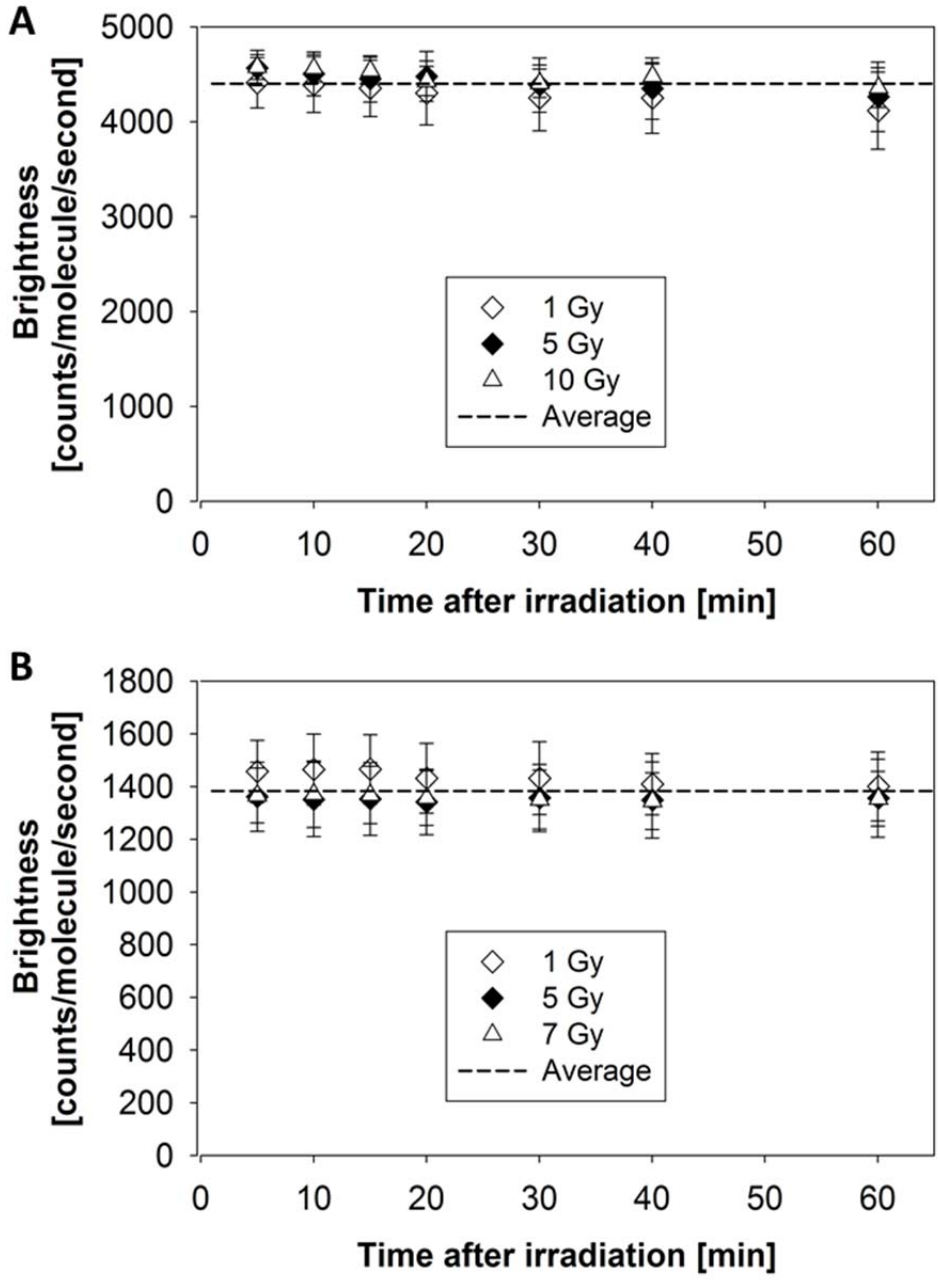

Figure S3: Relative changes in the mobile fraction of YFP-53BP1 protein as a function of time post-irradiation (left y-axis) are statistically indistinguishable from corresponding changes in relative fluorescence intensity (right y-axis) at both 1 Gy ($F(1,16)= 0.39$, $p= 0.55$) and 2 Gy ($F(1,16)= 0.016$, $p= 0.90$) γ-irradiation doses. The smooth curves show the fit to 1 Gy (dotted) and 2 Gy (solid) N&B analysis data. Each data point shows the mean and standard deviation of corresponding measurements from 10 cell nuclei.

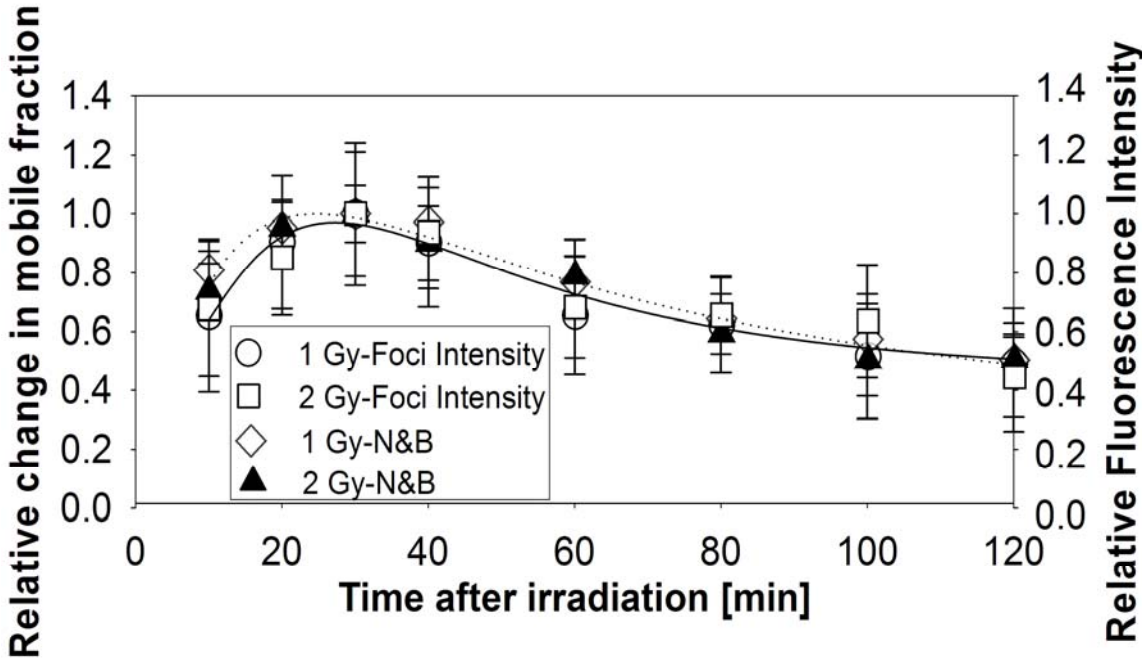

Figure S4: Strip-Fluorescence Recovery after Photobleaching (Strip-FRAP) used in calculating the ratio of mobile to immobile fraction needed to correct the results of N&B analysis. Strip-FRAP measurements on Xrs6 cells expressing GFP-Ku80, **(A)** as a function of time before and after 5 Gy of γ-irradiation, and **(B)** as a function of dose at 1 hr post-irradiation show both dose and time independence of the immobile fraction. Data sets were normalized to pre-bleach values.

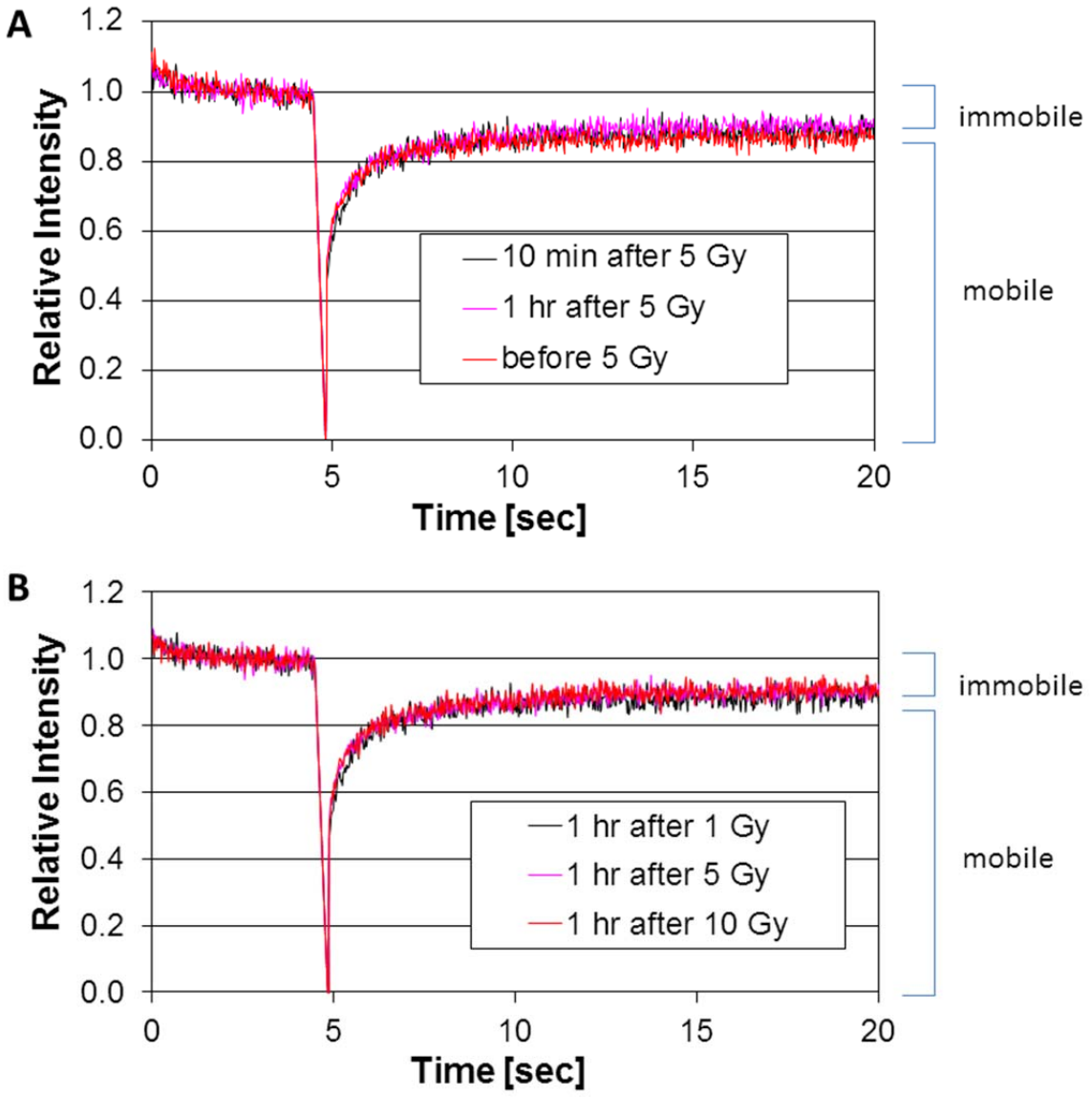

Figure S5: The need for methods to quantify sparse damage repair kinetics. Confocal images of YFP-53BP1 showed formation of foci after treatment with 100 μg/ml bleomycin (BLM, top row), while cells expressing GFP-Ku80 (middle row) and YFP-DNA-PKcs (bottom row) did not form foci after the same treatment.

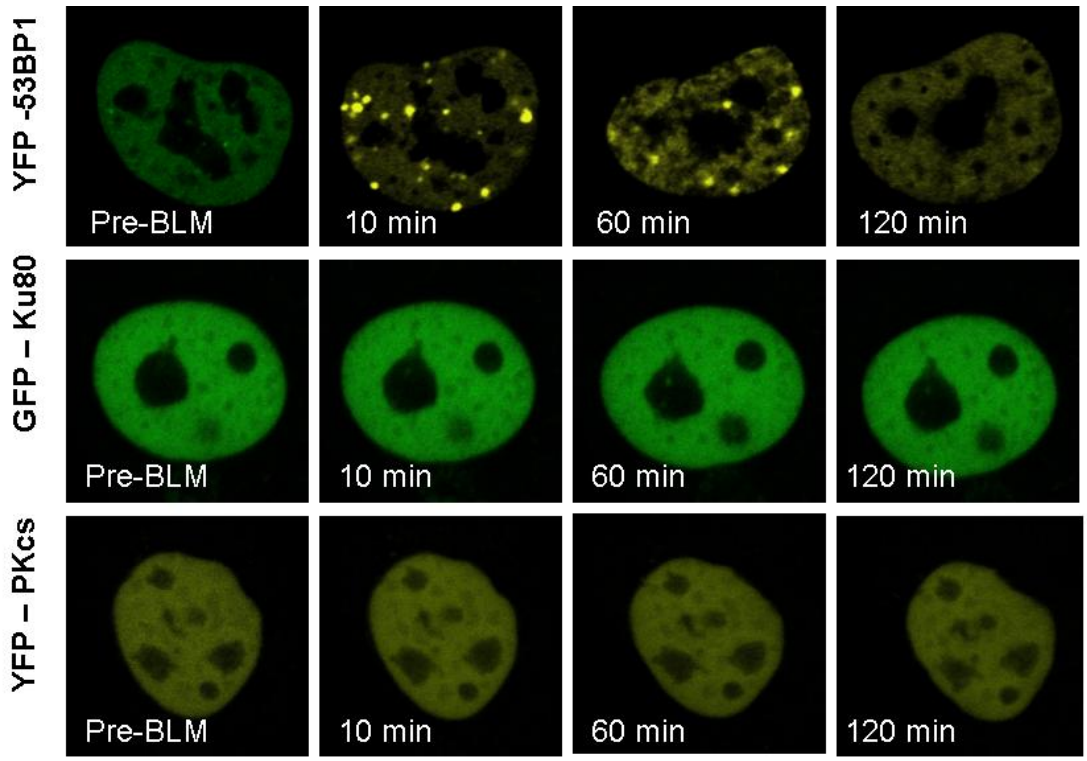

SUPPLEMENTARY REFERENCES

1. Magde, D., Webb, W.W. and Elson, E. (1972) Thermodynamic Fluctuations in a Reacting System - Measurement by Fluorescence Correlation Spectroscopy. *Physical Review Letters*, **29**, 705-&.
2. Elson, E.L. and Magde, D. (1974) Fluorescence Correlation Spectroscopy .1. Conceptual Basis and Theory. *Biopolymers*, **13**, 1-27.
3. Magde, D., Elson, E.L. and Webb, W.W. (1974) Fluorescence Correlation Spectroscopy .2. Experimental Realization. *Biopolymers*, **13**, 29-61.
4. Schwille, P., Haupts, U., Maiti, S. and Webb, W.W. (1999) Molecular dynamics in living cells observed by fluorescence correlation spectroscopy with one- and two-photon excitation. *Biophys J*, **77**, 2251-2265.
5. Koppel, D.E., Axelrod, D., Schlessinger, J., Elson, E.L. and Webb, W.W. (1976) Dynamics of Fluorescence Marker Concentration as a Probe of Mobility. *Biophysical Journal*, **16**, 1315-1329.
6. Rigler, R. and Ehrenberg, M. (1976) Fluorescence Relaxation Spectroscopy in Analysis of Macromolecular Structure and Motion. *Quarterly Reviews of Biophysics*, **9**, 1-19.
7. Kim, S.A., Heinze, K.G. and Schwille, P. (2007) Fluorescence correlation spectroscopy in living cells. *Nature Methods*, **4**, 963-973.